The Plant Cell, Vol. 15, 1242–1256, May 2003, www.plantcell.org © 2003 American Society of Plant Biologists

The GTPase ARF1p Controls the Sequence-Specific Vacuolar Sorting Route to the Lytic Vacuole

Peter Pimpl, Sally L. Hanton, J. Philip Taylor, Luis L. Pinto-daSilva, and Jürgen Denecke[1]

Centre for Plant Sciences, Faculty of Biological Sciences, University of Leeds, Leeds LS2 9JT, United Kingdom

We have studied the transport of soluble cargo molecules by inhibiting specific transport steps to and from the Golgi apparatus. Inhibition of export from the Golgi via coexpression of a dominant-negative GTP-restricted ARF1 mutant (Q71L) inhibits the secretion of α-amylase and simultaneously induces the secretion of the vacuolar protein phytepsin to the culture medium. By contrast, specific inhibition of endoplasmic reticulum export via overexpression of Sec12p or coexpression of a GTP-restricted form of Sar1p inhibits the anterograde transport of either cargo molecule in a similar manner. Increased secretion of the vacuolar protein was not observed after incubation with the drug brefeldin A or after coexpression of the GDP-restricted mutant of ARF1 (T31N). Therefore, the differential effect of inducing the secretion of one cargo molecule while inhibiting the secretion of another is dependent on the GTP hydrolysis by ARF1p and is not caused by a general inhibition of Golgi-derived COPI vesicle traffic. Moreover, we demonstrate that GTP-restricted ARF1-stimulated secretion is observed only for cargo molecules that are expected to be sorted in a BP80-dependent manner, exhibiting sequence-specific, context-independent, vacuolar sorting signals. Induced secretion of proteins carrying C-terminal vacuolar sorting signals was not observed. This finding suggests that ARF1p influences the BP80-mediated transport route to the vacuole in addition to transport steps of the default secretory pathway to the cell surface.

INTRODUCTION

Protein sorting by the secretory pathway is in many cases dependent on the budding of coated vesicles from the Golgi apparatus, which then fuse with their target membranes. In plants, these include the endoplasmic reticulum (ER) to recycle ER residents that have been lost via bulk flow (Pimpl et al., 2000; Phillipson et al., 2001), the prevacuolar compartment for proteins destined for the lytic vacuole (da Silva Conceicao et al., 1997), the storage vacuole (Hinz et al., 1999), and the plasma membrane (Geelen et al., 2002).

The general mechanism of vesicular transport is based on the budding of vesicles driven by the recruitment of coat proteins to the donor membrane, followed by their assembly to a structure that imposes a curvature. The assembly of the coat, followed by fission of the vesicle, coat dissociation, and finally vesicle fusion with the target membrane, are regulated by a variety of proteins. The best characterized coats include those containing clathrin and the nonclathrin types COPI and COPII, all of which contain multiple protein subunits (Robinson et al., 1998).

To achieve recycling of essential components, cells often use a GTPase cycle that permits the transient storage of energy within the conformation of proteins. In the case of the nonclathrin-coated vesicles, an activated GTP-bound form of a GTPase promotes the recruitment of coat components to the donor membrane and triggers vesicle budding. GTP hydrolysis then induces conformational changes in the coat complexes, which leads to coat dissociation. The energy is stored in the conformation of the coat proteins and is used to start a new cycle of coat recruitment and assembly. Activation of the GTPase occurs through the action of a specific guanine nucleotide exchange factor (GEF) that promotes the exchange of GDP for GTP on the GTPase. Likewise, GTP hydrolysis is stimulated by a GTPase-activating protein. Interference with any of these processes can lead to the collapse of the cycle and block a defined transport step in the secretory pathway.

The GTPase Sar1p initiates the recruitment of the COPII coat to the ER membrane, whereas the GTPase ARF1p (ADP ribosylation factor) performs a similar function for Golgi-derived COPI vesicle budding. Evidence for ER-derived COPII-dependent transport to the Golgi in plants arose from the coexpression of a GDP-trapped mutant of the GTPase rab1 (Batoko et al., 2000), a GTP-trapped form of the GTPase Sar1p (Takeuchi et al., 2000), and overexpression of the Sar1-specific GEF Sec12p (Phillipson et al., 2001). The COPII and COPI transport routes that control the traffic of proteins between the ER and the Golgi are expected to depend on each other because of the necessary recycling of vesicle transport machinery. Inhibition of one transport route may lead to the collapse of its matching retrograde route and vice versa (Batoko et al., 2000; Takeuchi et al., 2000; Phillipson et al., 2001).

Evidence for the existence of COPI in plants was demonstrated using cell fractionation, biochemical reconstitution assays, and electron microscopy (Movafeghi et al., 1999; Contreras et al., 2000; Pimpl et al., 2000). The GTPase ARF1p was shown to influence ER-to-Golgi transport as well as Golgi-derived transport to the plasma membrane, dependent on the cargo molecule (Lee et al., 2002; Takeuchi et al., 2002). Unlike the defined

[1] To whom correspondence should be addressed. E-mail j.denecke@leeds.ac.uk; fax 44-113-3432835.

Article, publication date, and citation information can be found at www.plantcell.org/cgi/doi/10.1105/tpc.010140.

specificity between Sec12p and Sar1p, there is a complex variety of ARF-GEFs (Moss and Vaughan, 1998); at present, the ARF specificity is not understood for the variety of predicted ARF-GEFs in the Arabidopsis genome databases. The best characterized plant ARF-GEF is the EMB30/GNOM gene product (Grebe et al., 2000; Shevell et al., 2000), and a recent report suggests its function in endosomal trafficking (Geldner et al., 2003).

Golgi-derived anterograde transport is characterized only with respect to vacuolar sorting. The two best characterized vacuolar sorting signals are the sequence-specific (NPIRL-like) sorting signals and the C-terminal vacuolar sorting signals, which show no defined consensus sequence but are located strictly at the C terminus (Neuhaus and Rogers, 1998).

Transport to the lytic vacuole in plants occurs via the prevacuolar compartment, an equivalent of the endosome in mammals and yeast (da Silva Conceicao et al., 1997; Sanderfoot et al., 1998; Bassham and Raikhel, 2000). The plant vacuolar sorting receptor (BP80/AtELP; for brevity, referred to as BP80 hereafter) is specific for the NPIRL-like signals. BP80 is enriched in clathrin-coated vesicle fractions (Kirsch et al., 1994) and has been located in the *trans*-Golgi and the prevacuolar compartment (Sanderfoot et al., 1998; Miller et al., 1999; Li et al., 2002). There also is functional evidence that BP80 shares common features with the VPS10 gene product in yeast (Humair et al., 2001). By analogy, it is likely that it is recycled from the prevacuolar compartment to the *trans*-Golgi via retromer-mediated transport (Seaman et al., 1997, 1998; Pfeffer, 2001). The retromer is believed to constitute a novel type of vesicle coat distinct from clathrin, COPI, or COPII, the components of which (VPS5, VPS17, VPS26, VPS29, and VPS35) are found in the Arabidopsis genome database.

Transport to the protein storage vacuole is thought to be a plant-specific phenomenon, and several lines of evidence suggest that this transport is biochemically distinct from transport to the lytic vacuole via sequence-specific sorting signals (Gomez and Chrispeels, 1993; Hoh et al., 1995; Matsuoka et al., 1995; Hohl et al., 1996; Paris et al., 1996; Hinz et al., 1999; Hillmer et al., 2001). The situation is complicated further by the fact that functionally different vacuolar compartments can fuse with each other (Paris et al., 1996), which explains how proteins with completely different sorting signals have been colocalized to the same vacuolar compartment (Schroeder et al., 1993).

In this study, we performed cargo transport experiments based on quantitative analysis of the reporter proteins in the cells and in the culture medium. We compared the transport of secretory proteins with that of vacuolar proteins and focused on soluble cargo molecules. To observe differential effects on the sorting of these molecules in vivo, we inhibited the COPII-dependent ER export route as well as the COPI-dependent Golgi export pathway. Interestingly, coexpression of a GTP-restricted mutant of the GTPase ARF1p caused a vacuolar protein to be secreted to the culture medium, whereas the transport of a secreted protein was inhibited. A comparison of different vacuolar cargo molecules revealed that this induced secretion was restricted to proteins that exhibit sequence-specific vacuolar sorting signals. These data suggest that ARF1p not only controls COPI transport but also influences the BP80-mediated route to the lytic vacuole.

RESULTS

Interference with ARF1p-Dependent Transport Causes Missorting of a Vacuolar Protein

It was demonstrated previously that ER-to-Golgi transport can be inhibited by overexpression of Sec12p or coexpression of the trans-dominant-negative mutant of the GTPase Sar1p carrying a point mutation (H74L) that interferes with GTP hydrolysis (Takeuchi et al., 2000; Phillipson et al., 2001). To extend the available tools, we also generated an equivalent trans-dominant-negative mutant of ARF1p carrying a point mutation (Q71L) that is GTP restricted (Pepperkok et al., 2000) and thus belongs to a similar class of mutation as the H74L mutant of Sar1p.

Sec12p and Sar1p (d'Enfert et al., 1992) can be detected in electroporated tobacco protoplasts and distinguished from the endogenous tobacco gene products when expression is high (Phillipson et al., 2001). Figure 1A shows the results of a transient expression experiment in which a constant amount of a plasmid encoding the secretory protein α-amylase was cotransfected with either ARF1p- or ARF1(Q71L)p-encoding plasmids. The secretion index was determined by quantifying the α-amylase activity in the medium and in the cells and calculating the activity ratio of medium to cells. Interestingly, overexpression of wild-type ARF1p did not influence α-amylase secretion, whereas the GTP-restricted mutant had a very strong inhibitory effect. This was observed for the GTPase Sar1p as well, which affects secretion only when the mutant form is cotransfected (Phillipson et al., 2001). We conclude that ARF1p can influence the anterograde secretory route to the cell surface. The detection of overexpressed Arabidopsis ARF1p is possible only when using high plasmid concentrations. This is attributable to the higher degree of conservation of ARF1 compared with Sar1 or Sec12 among eukaryotes (Pimpl et al., 2000), which causes the detection of endogenous tobacco ARF1p, unlike the endogenous tobacco Sar1p or Sec12p.

Figure 1B demonstrates the dominant-negative nature of the mutant. Cotransfection of an equal amount of wild-type ARF1-encoding plasmid and mutant ARF1 had hardly any effect on the inhibitory action of the mutant. When the concentration of wild-type ARF1p-encoding plasmid was increased, a reconstitution of secretion became more obvious, although even with 100-fold higher dosage compared with the mutant the recessive wild-type protein did not fully displace mutant ARF1 from its site of action. These experimental results correspond well with those obtained for Sar1(H74L)p and wild-type Sar1p (Phillipson et al., 2001).

We next wanted to compare the influence of cotransfected Sec12p-, Sar1(H74L)p-, and ARF1(Q71L)p-encoding plasmids on the two cargo molecules α-amylase and phytepsin. The vacuolar form of phytepsin can be distinguished easily from its precursor, which is in transit through the ER and the Golgi. Cleavage of the N-terminal propeptide was shown to occur in the lytic compartment or in a post-Golgi prevacuolar compartment. Moreover, saturation of vacuolar transport leads to missorting of the unprocessed precursor to the cell surface (Törmäkangas et al., 2001). This allows us to distinguish be-

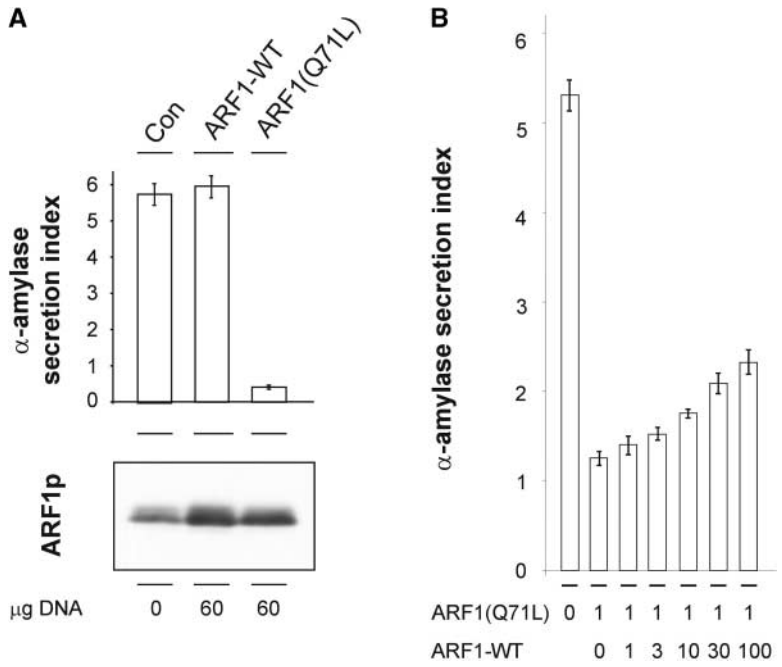

Figure 1. Transient Expression of Recombinant ARF1p and ARF1(Q71L)p in Tobacco Protoplasts.

(A) Coexpression of the secretory marker α-amylase with either wild-type ARF1p (ARF1-WT) or mutant ARF1(Q71L)p. The top panel shows the secretion index for α-amylase under control conditions (Con) compared with the coexpressed ARF1 proteins. The bottom panel shows the total amount of endogenous ARF1p (Con) compared with the higher protein level when 60 μg of wild-type ARF1 or ARF1(Q71L)-encoding plasmid was electroporated. Note the profound effect of the mutant GTPase on α-amylase secretion in contrast to the wild-type GTPase.
(B) Coexpression of the secretory marker with ARF1(Q71L)-encoding plasmid with a dilution series of wild-type ARF1-encoding plasmid. Annotations are as in **(A)**, and the amounts of plasmids are indicated in micrograms below the lanes.

tween three distinct populations of this cargo molecule: the precursor in transit, the processed vacuolar form, and the secreted precursor in the medium. Expressing a constant amount of cargo molecule, the effect of increasing the effector dosage was analyzed in tobacco leaf protoplast suspensions.

Figure 2 shows the dosage-dependent effect of the three effector molecules on the transport of our two cargo molecules. Whereas α-amylase secretion was inhibited by all effector molecules in a similar manner, the vacuolar protein phytepsin was influenced in a different way: (1) Overproduction of Sec12p led to an accumulation of unprocessed precursor in the cells and an inhibition of phytepsin secretion. Transport to the vacuole was less affected, as seen by a constant signal of the processed vacuolar form unless high concentrations of Sec12p-encoding plasmids were cotransfected. (2) Coexpression of Sar1(H74L)p led to a similar effect on secretion but a more noticeable inhibition of vacuolar sorting, as estimated from the diminishing signal of the processed form. (3) In contrast to the two former effectors, coexpression of ARF1(Q71L)p caused an increase in the secretion of phytepsin at an intermediate effector dosage. Moreover, transport to the vacuole was inhibited strongly, as shown by the rapid decline of the processed form at low effector concentrations.

The increase in phytepsin secretion was observed at intermediate concentrations of the ARF1 mutant at which α-amylase secretion already was inhibited significantly (Figure 2, 0.3 μg of DNA; compare phytepsin data with the secretion index of α-amylase). However, at higher concentrations of ARF1(Q71L)p, this secretion was reduced again to starting levels, whereas the processed vacuolar form became undetectable and the precursor was abundant in the cells. Our interpretation of these data is that ARF1(Q71L)p inhibits both secretion and vacuolar transport but that the latter is inhibited with greater sensitivity, giving rise to an apparent increase in secretion via the default route at intermediate concentrations of the effector.

Neither the Drug Brefeldin A Nor the GDP-Restricted ARF1 Mutant (T31N) Mimics the Effect of ARF1(Q71L)

To test our hypothesis, we wanted to compare the effect of ARF1(Q71L)p coexpression with that of other means to disrupt export from the Golgi apparatus. The drug brefeldin A (BFA) stabilizes an abortive complex with the GDP-bound form of ARF1p that has its GEF at the Golgi membrane (Chardin and McCormick, 1999; Peyroche et al., 1999). This effect leads to an inhibition of further ARF1p and coatomer recruitment to the Golgi apparatus (Pimpl et al., 2000; Ritzenthaler et al., 2002) and finally inhibits COPI vesicle formation itself. Therefore, BFA is expected to inhibit Golgi export in a different manner from the GTP-restricted ARF1(Q71L). Thus, we investigated the effect of increasing BFA concentrations on the transport of phytepsin.

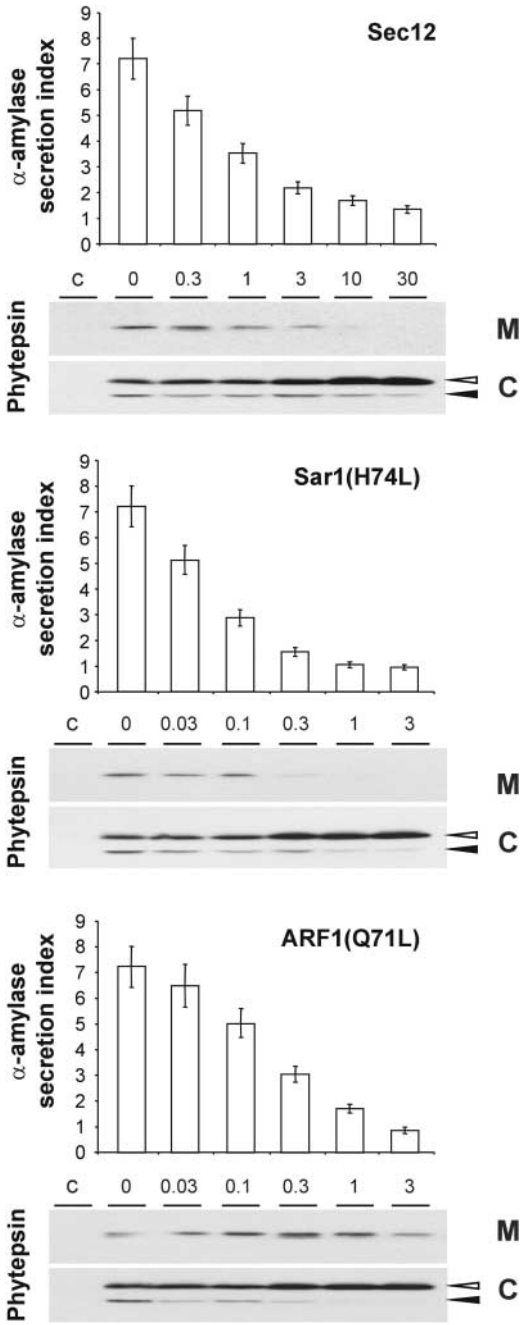

Figure 2. Manipulation of Secretion and Vacuolar Transport via the Key Molecules Sec12p, Sar1p, and ARF1p.

Transient expression in tobacco protoplasts. The secretory marker α-amylase or the vacuolar protein phytepsin was coexpressed with increasing concentrations of Sec12-, Sar1(H74L)-, or ARF1(Q71L)-encoding plasmids. The effector plasmid concentrations are given below each lane in micrograms. Mock-electroporated samples were used as blanks for all α-amylase assays (cells and medium) and are shown for phytepsin gel blots in a separate lane (c). Secretion index values for α-amylase are given in white bars, with standard errors indicated for five independent experiments. For phytepsin, equal volumes of medium (M) and cell (C) samples are compared by protein gel blot analysis. The white arrowhead denotes the unprocessed phytepsin precursor, and the black arrowhead denotes the processed vacuolar form of phytepsin devoid of the N-terminal propeptide (Törmäkangas et al., 2001). Note that all effector molecules cause a dosage-dependent inhibition of α-amylase secretion, whereas secretion of the unprocessed phytepsin precursor to the culture medium is induced specifically by ARF1(Q71L) coexpression.

The experiment was performed by pooling seven standard transfections with plasmids encoding either α-amylase or phytepsin, subdivision into seven equal populations, and supplementation with BFA to reach the indicated concentration of the drug. Figure 3 shows that BFA inhibited phytepsin precursor secretion and intracellular precursor processing to the lower molecular mass vacuolar form. The inhibition of the secretion was in sharp contrast to the induced secretion seen with ARF1(Q71L)p coexpression. Vacuolar sorting of phytepsin was abolished effectively by the drug, even at the lowest concentration applied. This finding suggests that BFA interferes with ARF1p-mediated transport in a different manner compared with ARF1(Q71L)p.

The secretion of α-amylase was reduced gradually with increasing concentrations of the drug. Moreover, total α-amylase activity was reduced by high BFA concentrations, whereas phytepsin recovery was unaffected. We have shown previously that BFA treatment for extended periods can reduce secretory protein synthesis on the rough ER, possibly as a result of the formation of the "BFA compartment" (Crofts et al., 1999). Also, in the experiment represented in Figure 2, the two GTPase mutants caused a threefold reduction of total α-amylase activity (data not shown), but the phytepsin yield appeared to be more or less constant. In all of these cases, the lower phytepsin synthesis was possibly compensated by greater stability caused by the prevention of vacuolar transport.

To extend our analysis of the role of ARF1p in Golgi export, we constructed a GDP-restricted form of ARF1 (T31N). This mutant is expected to mimic the BFA effect but may be more effective, because not all ARF-GEFs are BFA sensitive (Chardin et al., 1996; Moss and Vaughan, 1998). A constant amount of plasmids encoding α-amylase and phytepsin was cotransfected with increasing concentrations of ARF1(T31N)p-encoding plasmid. Figure 4 shows that ARF1(T31N)p effectively inhibited the secretion of the secretory marker α-amylase and reduced the total amount of the enzyme, as seen for the drug BFA. Likewise, phytepsin secretion was inhibited with increasing dosage of the effector, as was the level of the processed vacuolar form. By contrast, there was no apparent reduction of the total amount of phytepsin, again probably as a result of a rescue from the lytic vacuole.

In conclusion, neither treatment induced the transient phytepsin secretion observed for ARF1(Q71L)p coexpression. Because the effects on the anterograde transport of α-amylase were similar for both ARF1 mutants, the specific phytepsin secretion shown in Figure 2 cannot be explained by a general disruption of Golgi function. By contrast, the data suggest an ac-

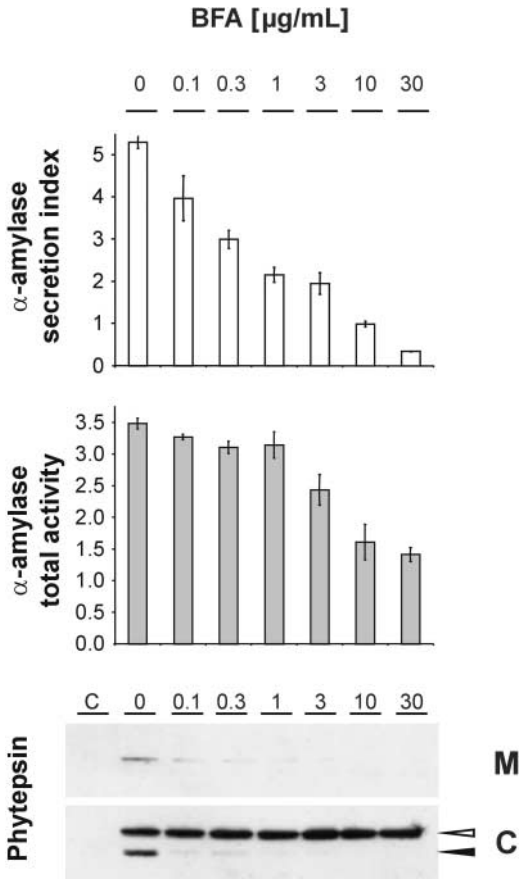

Figure 3. Influence of BFA on the Transport of α-Amylase and Phytepsin.

Transient expression experiment with tobacco protoplasts incubated with increasing concentrations of the drug BFA. The final concentration is indicated above each lane in micrograms per milliliter. Shown are the α-amylase secretion index (white bars) and total (cells plus medium) α-amylase activity per milliliter of cell suspension (gray bars) compared with phytepsin gel blots of medium (M) and cell (C) samples. Error bars are indicated for five independent experiments. The phytepsin precursor and processed form are annotated as in Figure 2. BFA inhibits α-amylase secretion, phytepsin secretion, and intracellular processing of phytepsin. Note that an induced secretion of phytepsin was not observed.

tive role of ARF1p-mediated GTP hydrolysis in the vacuolar sorting of phytepsin.

ARF1(Q71L)p-Induced Secretion Occurs through Specific Inhibition of Transport to the Lytic Vacuole

Plants contain more than one vacuolar compartment that are reached via different pathways depending on a variety of sorting signals (Hoh et al., 1995; Paris et al., 1996; Neuhaus and Rogers, 1998). Although it has been shown that barley phytepsin is detected in both lytic and storage vacuoles (Paris et al., 1996), it is still unclear which type of vacuolar sorting signal is present in phytepsin (Törmäkangas et al., 2001). For this reason, we wanted to test two established vacuolar sorting signals that are transplantable and that can redirect cargo molecules from the default pathway to vacuolar compartments.

We fused the C-terminal processed fragment of barley lectin (Bednarek and Raikhel, 1991) and the N-terminal propeptide of sweet potato sporamin (Koide et al., 1997) to the C terminus of α-amylase (Figure 5A), which was shown previously to maintain enzymatic activity upon fusion of small peptides (Crofts et al., 1999). The sporamin propeptide was shown to act as a sequence-specific vacuolar sorting signal regardless of its location within the protein (Koide et al., 1997) and was predicted to act properly at the C terminus of α-amylase. By contrast, the barley lectin propeptide has no sequence consensus but must be localized strictly at the C terminus (Dombrowski et al., 1993) and also can be transplanted to cargo molecules as long as its C-terminal exposure is not compromised (Rojo et al., 2002). The α-amylase fusion with the sporamin propeptide (amy-spo) would be predicted to act as a BP80 ligand (Koide et al., 1997; Matsuoka and Nakamura, 1999), whereas the fusion with the barley lectin propeptide (amy-bl) would be transported in a different manner (Matsuoka et al., 1995).

Figure 5B shows that both C-terminal fusions (amy-spo and amy-bl) were retained in the cells compared with amylase but that the fusion with the barley lectin propeptide exhibited some leakage to the medium. The latter effect corresponds to the incomplete cell retention that has been observed for other C-terminal vacuolar sorting signals, such as the chitinase propeptide or the AFVY motif of phaseolin (Neuhaus et al., 1994; Frigerio et al., 1998). No significant saturation of the targeting machinery was seen for amy-spo, indicating either greater efficiency or a greater capacity of the underlying sorting pathway.

To confirm the functionality of these two sorting signals in the context of the α-amylase C terminus, we conducted further control experiments. First, we tested the reported role of the large alkyl side chains within the NPIRL motif (Matsuoka and Nakamura, 1999) by Gly replacement, yielding NPGRG (amy-spoM). Figure 5B demonstrates that intracellular retention was abolished almost completely by this modification and illustrates the sequence-specific nature of this type of sorting signal (Neuhaus and Rogers, 1998; Matsuoka and Neuhaus, 1999). Second, the addition of double glycines to the C terminus of the barley lectin propeptide rendered this signal nonfunctional (Dombrowski et al., 1993; Rojo et al., 2002) in the case of our α-amylase fusion (amy-blGG). These control experiments were important because they demonstrate that the two different sorting signals exhibited all of the expected features when fused to α-amylase as a carrier.

We then tested whether the partial retention of amy-bl was attributable to the saturation of the sorting receptor. This was determined using a time-course experiment over a period of 30 h, which permitted us to compare the secretion profiles of amy, amy-spo, and amy-bl. For each cargo molecule, 20 standard transfections were pooled and split into 10 identical samples for time-resolved analysis. Figure 6 shows that α-amylase secretion took place during the entire course of the experiment and accounted for most of the total activity, as shown previously (Phillipson et al., 2001). By contrast, cellular retention of amy-bl was nearly complete during the first 6 h of the time course. After 9 h of incubation, secretion became detectable,

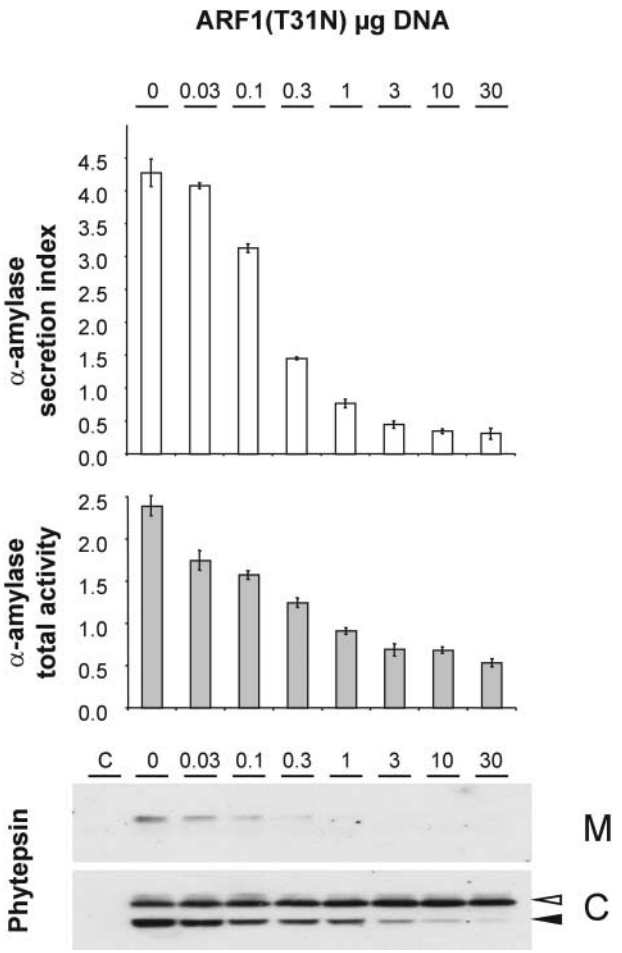

Figure 4. Influence of ARF1(T31N) on the Transport of α-Amylase and Phytepsin.

Transient expression in tobacco protoplasts. The secretory marker α-amylase or the vacuolar protein phytepsin was coexpressed with increasing concentrations of the plasmid encoding the GDP-restricted mutant of ARF1 (T31N). The plasmid concentration is indicated above each lane in micrograms. Shown are the α-amylase secretion index (white bars) and total (cells plus medium) α-amylase activity per milliliter of cell suspension (gray bars) compared with phytepsin gel blots of medium (M) and cell (C) samples. The phytepsin precursor and processed form are annotated as in Figure 2. ARF1(T31N) inhibits α-amylase secretion, phytepsin secretion, and intracellular processing of phytepsin and is comparable to the effect of BFA. In contrast to the effect of ARF1(Q71L) shown in Figure 2, ARF1(T31N) does not induce phytepsin secretion.

and after 20 h of incubation, intracellular amy-bl levels were constant, whereas secretion was comparable to that of amy. This effect also was deduced from the comparable slope of the total and medium amy-bl curves at time points 20, 24, and 30 h. We conclude that the partial secretion of amy-bl was not attributable to poor exposure of the sorting signal but to saturation of the transport machinery. In the same experiment, amy-spo was retained efficiently in the cells during the entire time course, confirming the lack of saturation seen in Figure 5B.

To determine if the secretion of these two cargo molecules would be induced by coexpression of ARF1(Q71L)p, as it was with the vacuolar protein phytepsin, transient coexpression experiments were performed using a constant amount of cargo molecules and an increasing dosage of ARF1(Q71L)p. Figure 7A shows that the secretion of amy-spo was stimulated by ARF1(Q71L)p, as observed for phytepsin. By contrast, ARF1(Q71L)p inhibited the secretion of amy-bl with increased dosage. Figure 7B shows the calculated secretion index, which demonstrates the completely opposite behavior of the two cargo molecules in response to the effector.

Another important observation was the differential influence of the effector molecule on the total activity of the cargo molecules. amy-bl levels decreased significantly with increasing ARF1(Q71L)p dosage, which also was observed for the secretory marker α-amylase (Figure 2; total activities not shown). By contrast, total amy-spo levels did not decrease, which also was observed for phytepsin (Figure 2). We postulate that the rescue from the lytic compartment and the resulting greater stability of phytepsin or amy-spo compensates for the negative physiological effect caused by ARF1(Q71L)p. We recreated the constructions illustrated in Figure 5A using green fluorescent protein instead of α-amylase as a cargo molecule and obtained identical results (S. Hanton and J. Denecke, unpublished data). We conclude that the ARF1(Q71L)-induced secretion is specific for cargo molecules carrying sequence-specific vacuolar sorting signals.

We also tested the mutagenized form of amy-spo containing the mutant motif NPGRG (amy-spoM). Figure 8A shows that secretion no longer was stimulated but in fact was inhibited by the ARF1 mutant. This finding confirms that induced secretion by the ARF1 mutant is a signature of sequence-specific sorting signals and thus BP80 ligands. Interestingly, a comparison of Figure 2 [ARF1(Q71L)p] with Figure 8A reveals that despite a similar secretion index of amy and amy-spoM, the secretion of amy was inhibited, whereas amy-spoM appeared to be unaffected unless very high levels of ARF1(Q71L)p were coexpressed. One explanation for this discrepancy is the possible residual vacuolar sorting of amy-spoM. Redirection of a small amount of amy-spoM from the vacuolar route to the cell surface could compensate for the anterograde transport inhibition observed with amy (Figures 1 and 2).

To test this hypothesis, we took advantage of the recent observation that the drug wortmannin inhibits both vacuolar sorting routes and not merely the route followed by proteins carrying C-terminal vacuolar sorting signals (Matsuoka and Neuhaus, 1999). Figure 8B shows that the secretion index of amy-spo was increased drastically (~100-fold). The secretion of amy or the retention of amy-HDEL was not affected significantly by the drug. The neutral behavior of these two control cargos demonstrates the specific action of the drug on the vacuolar sorting of amy-spo. Interestingly, the secretion of amy-spoM still was induced threefold by wortmannin, which can be explained by a weak residual vacuolar transport that was inhibited. Indeed, it appears from Figures 5B and 8B that amy-spoM was slightly less secreted than amy, although the difference was small. It is possible that the double point mutation does not abolish the interaction with the vacuolar sorting machinery completely.

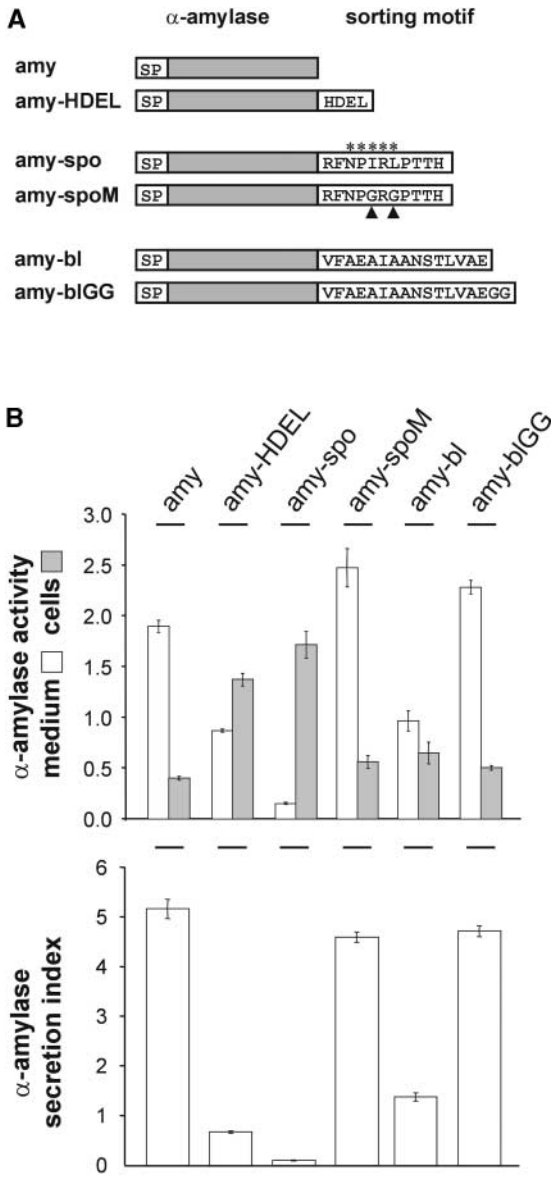

Figure 5. Propeptides of Sweet Potato Sporamin and Barley Lectin Are Functional at the C Terminus of α-Amylase.

(A) Scheme of the six cargo molecules: α-amylase (amy) and its derivatives carrying different C-terminal sorting motifs, including ER retention (amy-HDEL), two vacuolar sorting motifs (amy-spo and amy-bl), and mutated versions of both (amy-spoM and amy-blGG). The sequence-specific vacuolar sorting motif is highlighted by stars, and the two point mutations are indicated with arrowheads.

(B) Transient expression experiment showing a comparison of the six cargo molecules. The bottom panel shows the secretion index, and the top panel shows a direct comparison of extracellular (white bars) and intracellular (gray bars) α-amylase activity per milliliter of cell suspension. Note that the intracellular retention of amy-spo is almost complete compared with the leaky retention of amy-HDEL and amy-bl. Error bars are indicated for five independent experiments. Note also that the two mutants amy-spoM and amy-blGG are secreted with approximately similar efficiency as α-amylase.

We next wanted to determine whether the ARF1(Q71L)p-induced secretion of amy-spo was in fact the result of a lower level of vacuolar sorting. Because amy-spo does not exhibit a defined degradation intermediate such as phytepsin, it was necessary to assess vacuolar sorting by fractionation of vacuoles. The vacuolar marker α-mannosidase was used to normalize extracts from total cells and isolated vacuoles from the same cell suspensions. Protoplasts were transfected with amy-spo in the presence or absence of ARF1(Q71L)p or BFA. Proteins were extracted from the culture medium, total cells, and purified vacuoles. The secretion index was calculated, and we confirmed that ARF1(Q71L) induced secretion but the drug BFA did not (Figure 9, top). The α-amylase/α-mannosidase ratio was compared between cells and vacuoles from control incubations, cotransfection with ARF1(Q71L), and incubation in the presence of BFA (Figure 9, middle). The purity of the vacuolar fractions was tested using the ER resident marker calnexin, demonstrating that this marker did not copurify with α-mannosidase (Figure 9, bottom). To obtain an estimation of the degree of copurification between our cargo molecule and the vacuolar marker, the ratio was set to 100% in the total cell extracts. The result shows that amy-spo cofractionated with the vacuolar marker under control conditions but did so to a lesser extent in the presence of the two inhibitors. This finding demonstrates once again that both inhibitors compromise vacuolar sorting but only ARF1(Q71L)p induces the secretion of amy-spo.

It should be noted that the reduction of vacuolar sorting by these two inhibitors was less pronounced for amy-spo than for phytepsin, as deduced from the reduction of phytepsin precursor processing (Figures 2 and 3). This finding is particularly astonishing for the drug BFA, which generally inhibits vacuolar sorting efficiently in plants. However, it should be noted that the sorting pathway for α-mannosidase, which is not yet established in plants, may also be affected by the drug. If less α-mannosidase were transported to the vacuoles during the experiment, a higher α-amylase/α-mannosidase ratio would be the consequence. The apparent weaker inhibition of vacuolar sorting of amy-spo also may be explained by the greater sorting efficiency of amy-spo compared with phytepsin. Further experiments on the influence of BFA on ER export and the vacuolar sorting of amy-spo will be necessary to clarify this point.

DISCUSSION

ARF1p Controls the Golgi-Derived Transport of Phytepsin to the Vacuole

We inhibited transport between the ER and the Golgi using three different effector molecules that control different steps in this pathway. Overexpression of Sec12p is thought to inhibit ER-derived COPII vesicle budding itself through titration of the essential GTPase Sar1p (Nishikawa et al., 1994; Phillipson et al., 2001). By contrast, the primary effect of incorporating GTP-restricted forms of Sar1p or ARF1p is thought to be the formation of fusion-incompetent COPII or COPI vesicles (Nickel et al., 1998; Takeuchi et al., 1998; Pepperkok et al., 2000). Defective

GTP hydrolysis prevents uncoating of the vesicles, which then accumulate because they cannot fuse with their target membrane. This effect was deduced originally from in vitro transport assays using the nonhydrolyzable GTP analogs GTPγS and GMP-PNP (Melancon et al., 1987; Barlowe et al., 1994). In addition, it has been suggested that GTP hydrolysis influences cargo loading into nascent vesicles (Nickel et al., 1998; Pepperkok et al., 2000).

Because α-amylase is a naturally secreted protein, it follows the anterograde COPII route to the Golgi (Phillipson et al., 2001) and then to the cell surface by an unknown carrier. Although the mechanism of inhibition is different for the three effector molecules, the result appears to be identical, and the secretion of α-amylase is inhibited in a similar manner (Figure 2). This is particularly interesting for the GTP-restricted mutants of Sar1 and ARF1, because the first should specifically inhibit COPII transport, whereas the second should specifically inhibit COPI transport.

To explain the strong inhibition by ARF1(Q71L)p, two current models describing intra-Golgi transport (Pelham and Rothman, 2000; Pelham, 2001) can be discussed with respect to the role of COPI-mediated transport: the cisternal maturation model predicts an exclusive role of COPI in retrograde transport, whereas the vesicular transport model postulates the existence of two distinct populations of COPI vesicles, one for retrograde transport and one for anterograde transport. The inhibition of α-amylase secretion by ARF1(Q71L)p can be explained by either model. If the COPI route is exclusively retrograde and functions as a recycle pathway for ER residents and the COPII ER export machinery, then its inhibition would be expected to rapidly cause an indirect collapse of COPII-dependent ER export as well. Alternatively, if anterograde intra-Golgi transport occurs in a distinct COPI carrier, then ARF1(Q71L)p would inhibit the secretion of α-amylase at the Golgi level. Our data on the secretory cargo molecule alone do not distinguish between these two possibilities.

Therefore, we included phytepsin as a second soluble cargo molecule. Phytepsin, like α-amylase, leaves the ER in COPII vesicles (Törmäkangas et al., 2001) but deviates at the Golgi apparatus to reach the vacuole. This fact permitted us to conduct a direct comparison of experiments in which all factors were constant (the protoplast suspension, the incubation time, and the type and concentration of effector molecules) except for the cargo molecule (Figure 2). Sec12 overexpression and Sar(H74L) slowed the secretion and the vacuolar delivery of phytepsin in a dosage-dependent manner similar to that observed for amy. However, ARF1(Q71L)p coexpression inhibited vacuolar transport but stimulated the secretion of the unprocessed phytepsin precursor to the culture medium. This opposite effect was seen at concentrations of ARF1(Q71L)p at which the secretion of amy was inhibited significantly (Figure 2).

An ARF1(Q71L)p-mediated induction of phytepsin secretion and the simultaneous inhibition of α-amylase secretion cannot be explained by an indirect effect on COPII transport or by a general collapse of anterograde intra-Golgi transport. These effects can be explained only if ARF1p controls two distinct Golgi export steps, one of which must be specific for the vacuolar route.

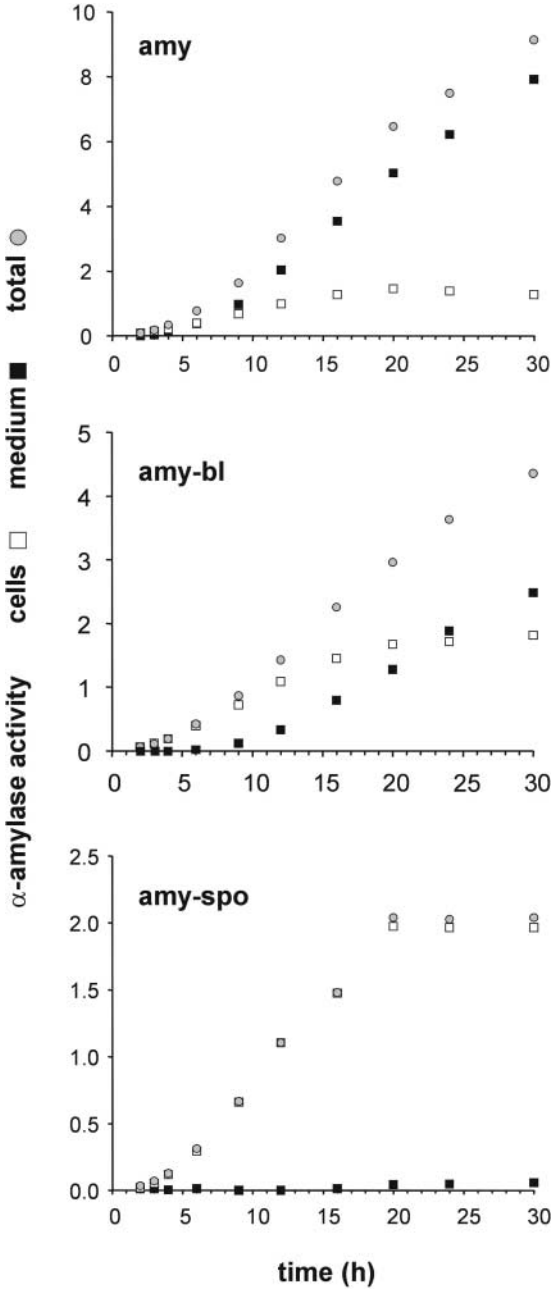

Figure 6. Leaky Retention of amy-bl Is Attributable to Saturation of the Sorting Pathway.

Transient expression experiment showing a time course for a period of 30 h to compare the transport of amy (top), amy-bl (middle), and amy-spo (bottom) as a function of time. Shown are the intracellular (white squares), extracellular (black squares), and total (gray circles) α-amylase activities per milliliter of suspension. Values are means from three measurements from a single time-course experiment. Note that the secretion of amy-bl starts only after an intracellular threshold level is reached (9 h of expression).

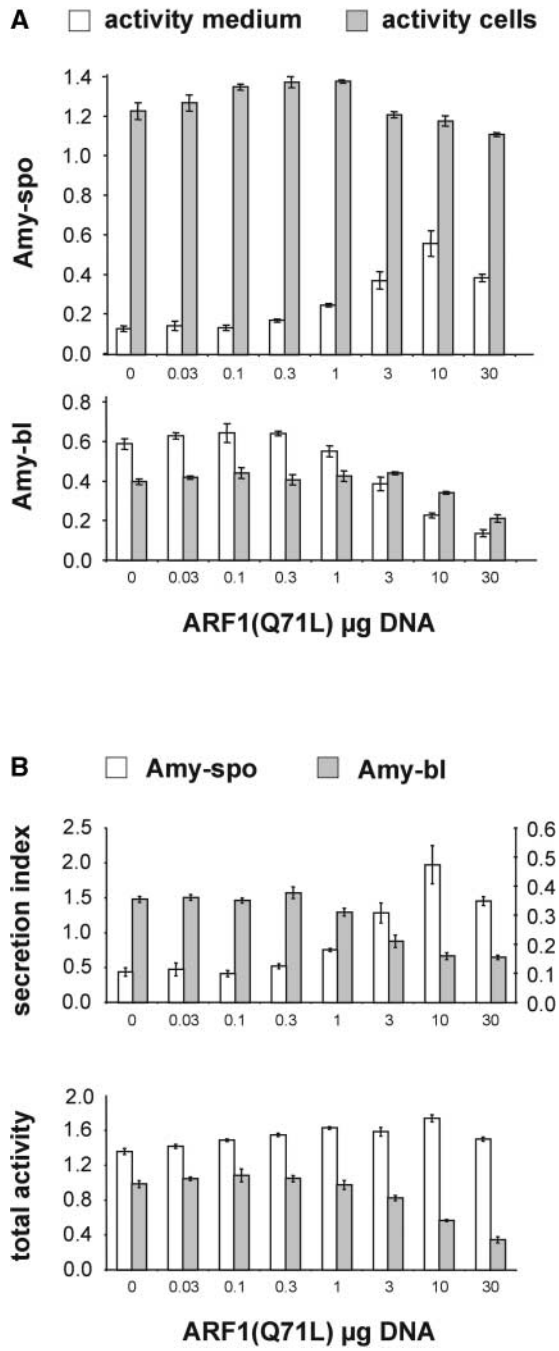

Figure 7. ARF1(Q71L)-Induced Secretion Occurs Specifically for Sequence-Specific Sorting Signals.

Transient expression experiment testing the influence of an increasing concentration of ARF1(Q71L)p on the transport of amy-spo and amy-bl. **(A)** Extracellular (white bars) and intracellular (gray bars) activities per milliliter of protoplast suspension are shown for amy-spo and amy-bl as a function of increased dosage of ARF1(Q71L)p. The plasmid concentration for the effector is given below each lane in micrograms. Error bars are indicated for five independent experiments. Note an increase in the extracellular level of amy-spo at high concentrations of ARF1(Q71L)p, in contrast to amy-bl, whose secretion diminishes under these conditions.

(B) Data from **(A)** represented as secretion index or total activity per milliliter of protoplast suspension for direct comparison between amy-spo and amy-bl. amy-spo is represented by white bars (right *y* axis for the secretion index) and amy-bl is represented by gray bars (left *y* axis for the secretion index). Error bars are indicated for five independent experiments. Note the opposite behavior of the secretion index for the two fusion proteins. Note also that the total amy-bl activity decreases with the increasing dosage of ARF1(Q71L)p, whereas that of amy-spo increases slightly.

According to the cisternal maturation model, ARF1p-regulated export from the Golgi would mediate vacuolar sorting in addition to its role in retrograde recycling. To explain the induced secretion of phytepsin, it is sufficient to postulate that the vacuolar route is more sensitive to the ARF1 mutant and collapses well before the indirect inhibition of COPII ER export. The vesicular transport model would require three roles for ARF1p-dependent Golgi steps: (1) retrograde recycling, (2) anterograde intra-Golgi transport of secretory cargo, and (3) anterograde Golgi export of vacuolar cargo. In addition, it also would be necessary to postulate that the vacuolar route is more sensitive to ARF1(Q71L)p than the two other routes combined.

The common denominator of both models is a role for ARF1p in vacuolar sorting and a high sensitivity of this route to an ARF1 mutant in which GTP hydrolysis is compromised. With high levels of ARF1(Q71L)p, ER-to-Golgi transport became so limited that the secretion of phytepsin started to diminish (Figure 2). Consistent with this finding, we found that very high ARF1(Q71L)p dosage caused intracellular retention of the phytepsin precursor (data not shown), which is consistent with the data obtained recently on a sporamin–green fluorescent protein fusion protein (Takeuchi et al., 2002).

ARF1p-Mediated GTP Hydrolysis Is Required for Efficient Vacuolar Sorting of Phytepsin

To study the mechanism by which ARF1p controls phytepsin sorting away from the secretory default pathway to the vacuole, we tested two other inhibitors that should target ARF1p-dependent transport steps. (1) The drug BFA is thought to titrate ARF1-GEF through the stabilization of an abortive GDP-ARF1p/ARF1-GEF complex (Chardin and McCormick, 1999; Peyroche et al., 1999) and to prevent ARF1p and coatomer recruitment to the Golgi apparatus and inhibit COPI vesicle formation (Pimpl et al., 2000; Ritzenthaler et al., 2002). (2) The GDP-restricted form of ARF1p(T31N) is expected to mimic a BFA-like effect and titrate ARF1-GEFs (Lee et al., 2002; Takeuchi et al., 2002). Unlike ARF1(Q71L), these two inhibitors should prevent vesicle budding itself.

Incubation in the presence of the drug BFA or coexpression of ARF1(T31N) did not cause induced secretion of phytepsin, although vacuolar sorting was impaired and the precursor accumulated in the cells (Figures 3 and 4). In these experiments, the secretory marker α-amylase also was retained in the cells in a dosage-mediated manner, similar to the data shown in Figure

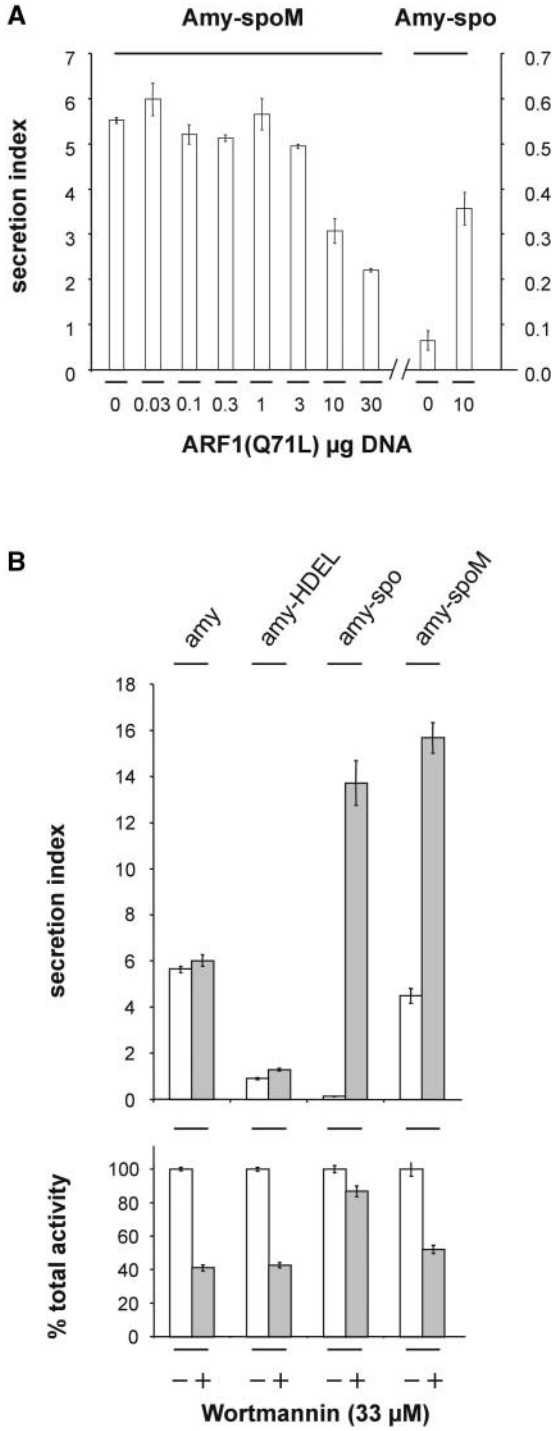

Figure 8. ARF1(Q71L)-Induced Secretion Is Dependent on the NPIRL Motif.

(A) Transient expression experiment showing the influence of an increasing concentration of ARF1(Q71L)p on the secretion index of amy-spoM (exhibiting the mutated sorting motif illustrated in Figure 5). The plasmid concentration of the effector is given below each lane in micrograms. The last two lanes represent a positive control carried using the same protoplasts, demonstrating the ability of ARF1(Q71L)p to induce secretion of the wild-type sporamin fusion. Error bars are indicated for five independent experiments. Note that none of the concentrations of ARF1(Q71L)-encoding plasmid leads to induced secretion of amy-spoM (cf. Figure 7B, secretion index for amy-spo).

(B) Influence of the drug wortmannin on the transport of cargo molecules in transient expression using tobacco leaf protoplasts. The following cargo molecules were compared under control conditions (white bars) or in the presence of wortmannin (gray bars): amy, amy-HDEL, amy-spo, and amy-spoM. Shown is either the secretion index (top) or the percentage of activity remaining after wortmannin treatment (bottom). Error bars are indicated for five independent experiments. Note the induced secretion of amy-spo and amy-spoM in response to the drug. Note also that the total activity is reduced by the drug in all samples except for amy-spo.

2. This quantitative comparison of both ARF1 mutants shows that ARF1p-mediated GTP hydrolysis must be an important step in the Golgi-derived transport to the vacuole and is particularly useful to dissect vacuolar transport from the more general anterograde route followed by secreted proteins such as α-amylase.

ARF1p Controls BP80-Mediated Transport to the Vacuole

Transport to the vacuoles in plants is complex as a result of the existence of two or more vacuolar compartments with different biochemical compositions and transport pathways (Paris et al., 1996). Therefore, it is of interest to study which of the known routes to the vacuole contains an ARF1-regulated transport step. The barley aspartic protease, referred to here as phytepsin, was chosen initially as a model cargo because it was shown to be a COPII cargo (Törmäkangas et al., 2001) and thus would serve best to compare with amy. Because phytepsin was shown to localize to either the lytic vacuole or the storage vacuole (Paris et al., 1996), it is plausible that it contains a BP80 sorting motif in addition to a second unrelated sorting motif, but this remains to be demonstrated (Törmäkangas et al., 2001). For this reason, we tested two of the best analyzed sorting signals in plants: the signal-specific vacuolar sorting signal of sweet potato sporamin (Koide et al., 1997, 1999; Matsuoka and Nakamura, 1999) and the C-terminal vacuolar sorting signal of barley lectin (Bednarek and Raikhel, 1991; Dombrowski et al., 1993). Sweet potato sporamin is transported in a BP80-mediated manner to the vacuole, as documented by the ability of NPIRL-like motifs to bind to BP80 in vitro and in vivo, whereas barley lectin does not interact directly with BP80 and reaches the vacuole in a different manner (Kirsch et al., 1994, 1996; Ahmed et al., 2000; Humair et al., 2001).

The two sorting signals were fused to the reporter α-amylase, because it accepts C-terminal fusions without the loss of enzymatic activity, analogous to the enzyme invertase, which has been instrumental in the generation of fusion proteins for vacuolar sorting studies in yeast (Robinson et al., 1988). We demonstrated via point mutagenesis of the BP80 binding motif (NPIRL to NPGRG) that the sporamin signal continued to act as a sequence-specific vacuolar sorting signal when fused to the

C terminus of α-amylase. Likewise, the barley lectin signal still acted as a C-terminal vacuolar sorting signal, because the addition of two more Gly residues rendered the signal nonfunctional (Figure 5B). The intracellular retention of amy-bl appeared to be very leaky, but we demonstrated that this effect was attributable to saturation rather than to poor functionality of the sorting signal (Figure 6), and it corresponds to previous findings on the saturation of C-terminal vacuolar sorting signals (Neuhaus et al., 1994; Frigerio et al., 1998). Interestingly, the intracellular retention of amy-spo was almost complete, which provides a new argument suggesting that it follows a different, less saturable transport route than amy-bl.

When the two engineered vacuolar forms of α-amylase were coexpressed with an increasing dosage of ARF1(Q71L)p, only the sporamin fusion exhibited the induced secretion seen for phytepsin (Figure 7). Therefore, our results suggest that ARF1p controls one of the steps in the BP80-mediated sorting pathway to the lytic vacuole. By analogy to phytepsin, the drug BFA did not show the induced secretion of amy-spo but caused less efficient vacuolar sorting, as observed for ARF1(Q71L)p (Figure 9). This finding confirms that it is ARF1p-mediated GTP hydrolysis, and not a general inhibition of ARF1p-dependent transport steps, that mediates vacuolar sorting.

Point mutagenesis of the BP80 binding motif (NPIRL to NPGRG) of amy-spo compromised not only vacuolar sorting but also ARF1(Q71L)p-induced secretion (Figure 8). This result links BP80 action to the observed ARF1(Q71L)p-induced secretion of phytepsin and amy-spo. Furthermore, the NPIRL-to-NPGRG mutation dramatically reduced the factor by which wortmannin induced the secretion of the α-amylase fusion. This drug caused a 100-fold induction of amy-spo secretion but only a 3-fold induction of amy-spoM secretion. It had no meaningful effect on the transport of the two control cargos, α-amylase and α-amylase-HDEL (Phillipson et al., 2001).

The two controls demonstrate how specific the action of wortmannin is on the plant secretory pathway. Neither secretion nor HDEL-mediated retention was affected by the drug, excluding the possibility that the inhibition of the sequence-specific vacuolar sorting pathway is an artifact. Wortmannin treatment led to an efficient redirection of vacuolar cargo to the cell surface via the default pathway, apparently without compromising ER export (Figure 10). This explains the more drastically induced secretion seen with ARF1(Q71L)p previously.

Interestingly, the residual threefold induction of amy-spoM secretion demonstrates that it does not behave like unmodified α-amylase. The inhibition of α-amylase secretion by ARF1(Q71L)p required a lower effector dosage than the inhibition of amy-spoM secretion [cf. Figure 8A with Figure 2, ARF1(Q71L)]. We postulate that amy-spoM still exhibited residual vacuolar sorting and that the NPIRL-to-NPGRG mutation was insufficient to block vacuolar sorting of the protein fusion completely. At a low dosage of ARF1(Q71L)p, inhibition of anterograde transport and redirection of vacuolar transport to the cell surface could compensate for each other. This finding could explain why a higher effector dosage is needed to inhibit the secretion of amy-spoM compared with the unmodified α-amylase.

The results from the comparison between sequence-specific and C-terminal sorting signals suggest that phytepsin follows the BP80 route. Phytepsin may not carry an obvious NPIRL-like motif, but it is clear that a number of variants of the NPIRL occur in nature and may not always be detected via sequence analysis (Matsuoka and Neuhaus, 1999). Also, phytepsin has been detected in two different types of vacuoles, one of which could be dependent on BP80-mediated sorting (Paris et al., 1996).

We conclude that the BP80-mediated transport to the lytic vacuole is controlled by ARF1p-mediated GTP hydrolysis. The recent discovery of ARF1 mutants in yeast showing aberrant secretion of the vacuolar protein carboxypeptidase Y and the

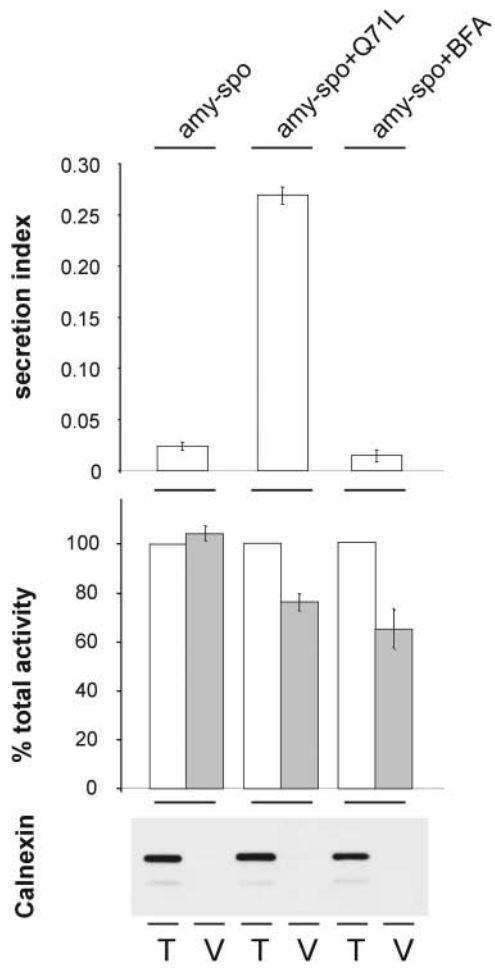

Figure 9. Vacuolar Sorting of amy-spo.

Transient expression experiment to illustrate the intracellular partitioning of amy-spo in control conditions or in the presence of ARF1(Q71L) or the drug BFA. Ten standard transfections were pooled for each condition; a portion was analyzed for the secretion index, and the remainder was analyzed for vacuolar sorting. The secretion index is shown at top. The α-amylase/α-mannosidase ratio is shown as a percentage of the total cell extract (set to 100%) to estimate the degree of amy-spo copurification with the vacuolar marker α-mannosidase. Error bars are indicated for five independent experiments. The protein gel blot (bottom) shows the amount of calnexin detected when equal amounts of α-mannosidase were loaded on SDS-polyacrylamide gels for total cell extracts (T) and purified vacuoles (V).

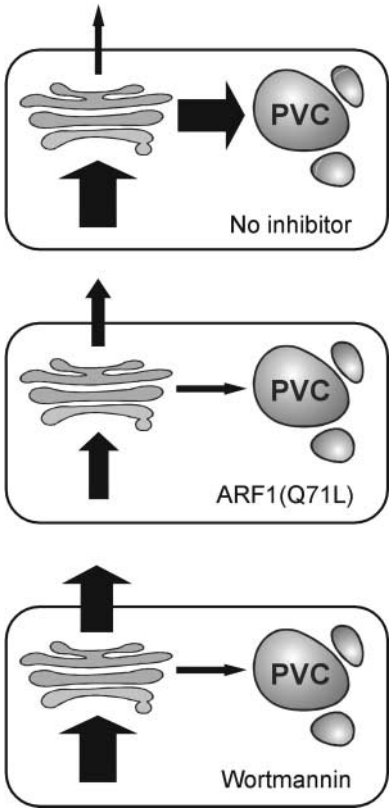

Figure 10. Model Illustrating the Effect of ARF1(Q71L)p and Wortmannin on Protein Transport.

Scheme illustrating the effect of ARF1(Q71L)p and wortmannin on ER export, Golgi export to the prevacuolar compartment (PVC), and Golgi export to the cell surface (black arrows). Under normal physiological conditions without inhibitors, the majority of vacuolar proteins are exported to the prevacuolar compartment and only a small fraction escapes to the cell surface because of receptor saturation. ARF1(Q71L)p inhibits both vacuolar transport and ER export, resulting in a modest induction of secretion of vacuolar proteins. By contrast, the drug wortmannin inhibits only the vacuolar sorting route and causes more pronounced secretion of vacuolar proteins.

ER resident protein BiP provides further evidence that ARF1 mutations can cause multiple mistargeting (Yahara et al., 2001). It will be interesting to test which of these yeast mutants are compromised in GTP hydrolysis. ARF1(Q71L)p-induced secretion of BP80 ligands provides a completely new assay to distinguish between two distinct vacuolar sorting pathways in plants and provides a new tool in addition to the differential wortmannin sensitivity (Matsuoka and Neuhaus, 1999).

How Can ARF1p Control Vacuolar Sorting?

The question remains how GTPase-deficient ARF1p coexpression leads to the compromised vacuolar sorting of BP80 ligands. In addition to its function in COPI-mediated transport, ARF1p also has been proposed to influence clathrin-coated vesicle formation via the recruitment of the adaptor complex (AP-1) to the *trans*-Golgi (Stamnes and Rothman, 1993). Consistently, BP80 was identified originally from purified clathrin-coated vesicles (Kirsch et al., 1994), and the cytosolic tail of an Arabidopsis BP80 isoform was shown to interact in vitro with the mammalian AP-1 clathrin-adapter complex (Sanderfoot et al., 1998). However, ARF1p was also implicated in an AP-1–independent recruitment of clathrin via the "GGA" protein family (Golgi-associated, γ-adaptin homologous, ARF-interacting proteins) (Puertollano et al., 2001). One of these clathrin-dependent pathways could be responsible for the delivery of BP80 ligands from the *trans*-Golgi to the prevacuolar compartment. Together, our new findings correspond well with a proposed role for ARF1p in BP80-mediated sorting in plants.

BP80 also is expected to recycle from the prevacuolar compartment back to the Golgi via an equivalent of the yeast retromer route (Seaman et al., 1997, 1998; Pfeffer, 2001). If the retromer route is inhibited, directly or indirectly, via mutant ARF1p coexpression, BP80 would progressively deplete in the *trans*-Golgi, leading to secretion of the BP80 ligands. Also, one of the plant ARF-GEFs, the GNOM gene product, was shown recently to be localized to the prevacuolar compartment (Geldner et al., 2003), but it remains to be determined which ARF family member interacts with this protein. However, there is no experimental evidence at present for the direct involvement of ARF1p in retromer-dependent transport, and further research will be required to determine how ARF1p-mediated GTP hydrolysis controls vacuolar sorting via the BP80 route.

METHODS

Plasmids for Transient Expression of Cargo Molecules

All DNA manipulations were performed according to established procedures. The *Escherichia coli* MC1061 strain (Casadaban and Cohen, 1980) was used for the amplification of all plasmids. Previously established plasmids encoding α-amylase and α-amylase-HDEL (Crofts et al., 1999) and phytepsin (Törmäkangas et al., 2001) were used. The four plasmids encoding the α-amylase derivatives amy-spo (pSLH44), amy-spoM (pSLH49), amy-bl (pSLH33), and amy-blGG (pSLH34) were generated by inserting annealed oligonucleotide pairs between the BglII and XbaI sites of the α-amylase–encoding plasmid that overlap with the last codon and the stop codon. The following oligonucleotide pairs were used to generate the C-terminally fused peptide-encoding regions: spo-sense (5′-GATCAGATTCAATCCCATCCGCCTCCCCACCACACACTAACT-3′) and spo-anti (5′-CTAGAGTTAGTGTGTGGTGGGGAGGCGGATGGGATTGAATCT-3′); spoM-sense (5′-GATCAGATTCAATCCCGGTCGCGGTCCCACCACACACTAACT-3′) and spoM-anti (5′-CTAGAGTTAGTGTGTGGTGGGACCGCGACCGGGATTGAATCT-3′); bl-sense (5′-GATCGTTTTTGCTGAAGCTATTGCTGCTAATTCTACTCTTGTTGCTGAATAAT-3′) and bl-anti (5′-CTAGATTATTCAGCAACAAGAGTAGAATTAGCAGCAATAGCTTCAGCAAAAAC-3′); blGG-sense (5′-GATCGTTTTTGCTGAAGCTATTGCTGCTAATTCTACTCTTGTTGCTGAAGGTGGATAAT-3′) and blGG-anti (5′-CTAGATTATCCACCTTCAGCAACAAGAGTAGAATTAGCAGCAATAGCTTCAGCAAAAAC-3′). Underlined areas represent point mutations or inserted codons. All constructions were verified by sequence analysis.

Plasmids for Transient Expression of Effector Molecules

The Sec12p overproduction plasmid was described previously (Phillipson et al., 2001). A new Sar1(H74L) overexpression plasmid (pPP11) was

created by subcloning the Sar1 coding region of pLL18 (Phillipson et al., 2001) as a ClaI-XbaI fragment into pLL4, which contains the 35S promoter of *Cauliflower mosaic virus*, a spacer DNA flanked by ClaI and XbaI sites overlapping with the translation initiation and stop codons, followed by the 3′ untranslated end of the nopaline synthase gene. An Arf1p-overexpressing plasmid (pPP5) was created by PCR-mediated amplification of the ARF coding region using the oligonucleotides ARF1-sense (5′-GATCACCATGGGGTTGTCATTCGG-3′) and ARF1-anti (5′-GCTAACTCTAGATCTATGCCTTGCTTGCGAT-3′) from first-strand cDNA prepared from 5-day-old seedlings of *Arabidopsis thaliana* according to established procedures (Denecke et al., 1995). To generate ARF1(Q71L), the following two oligonucleotides were used for site-directed mutagenesis of pPP5, ARF1MS (5′-GGGATGTTGGGGGTCTCGACAAGATCC-GTCCA-3′) and ARF1MA (5′-TGGACGGATCTTGTCGAGACCCCCAA-CATCCC-3′), resulting in the derived plasmid pLL20. To generate ARF1(T31N), the following two oligonucleotides were used for site-directed mutagenesis of pPP5, ARF1T31NS (5′-ATGCTGCTGGTA-AGAATACTATCCTCTACAAG-3′) and ARF1T31NA (5′-CTTGTAGAG-GATAGTATTCTTACCAGCAGCAT-3′), resulting in the derived plasmid pPP13. Underlined regions represent point mutations. All constructions were verified by sequencing.

Transient Expression and Plant Material

Tobacco plants (*Nicotiana tabacum* cv Petit Havana) (Maliga et al., 1973) were grown in Murashige and Skoog (1962) medium and 2% sucrose in a controlled room at 25°C with a 16-h daylength at a light irradiance of 200 $\mu E \cdot m^{-2} \cdot s^{-1}$. Preparation of tobacco leaf protoplasts and transfection via electroporation were performed as described previously (Phillipson et al., 2001), and the plasmid concentrations used are given in the figure legends. All incubations were performed for 24 h except for the time course shown in Figure 6. The harvesting of cells and culture medium was described previously (Phillipson et al., 2001; Törmäkangas et al., 2001). Brefeldin A was dissolved as a 20-mg/mL stock solution in DMSO and was diluted for protoplast incubation as indicated in the figure legends. Wortmannin was dissolved as a 33-mM stock solution in DMSO and diluted 1000-fold for final incubation of the protoplasts.

Protein Extraction and Gel Blot Analysis

Except for α-amylase assays, protein analysis of protoplast culture medium was performed after concentration with aqueous ammonium sulphate solution (60% final) in the presence of BSA as a carrier (200 μg per 600 μL of medium), resuspending the protein precipitate in phytepsin extraction buffer (Törmäkangas et al., 2001). Using this method, culture medium samples were concentrated 10-fold. Protein analysis of cells was conducted after sonication of the protoplasts in phytepsin extraction buffer in a 10-fold lower volume than the cell suspension.

Equal volumes of protein cell extracts or concentrated medium were supplemented with 2× SDS loading dye (Crofts et al., 1999) before boiling and gel loading. Protein analysis was performed by SDS-PAGE on 10 to 12% acrylamide gels. After gel blotting, immunodetection of phytepsin was performed with enhanced chemiluminescence using rabbit polyclonal antiserum raised against phytepsin at a 1:5000 dilution (Törmäkangas et al., 2001). Immunodetection of calnexin was performed similarly, except for a higher dilution (1:15,000) of the anti-calnexin serum (Pimpl et al., 2000).

Vacuole Preparation

Vacuoles were isolated from protoplasts at 24 h after electroporation in transient expression experiments as described (Törmäkangas et al., 2001), except for the omission of the cellulose synthesis inhibitor 2,6-dichlorobenzonitrile, which proved to be unnecessary.

Enzyme Assays

α-Amylase assays and calculation of the secretion index were performed as described (Crofts et al., 1999; Phillipson et al., 2001), except for those assays that were performed in conjunction with α-mannosidase assays, in which enzymes were first extracted in α-mannosidase extraction buffer and then diluted twofold with α-amylase extraction buffer to permit both enzyme assays to be performed on the same extracted material. α-Mannosidase assays for vacuolar partitioning experiments were performed as described previously (Törmäkangas et al., 2001) and were used for the quantification of vacuole recovery. Equal amounts of α-mannosidase activity were loaded for cells and purified vacuoles on SDS-polyacrylamide gels to analyze the levels of calnexin to control for endoplasmic reticulum contamination in the vacuole preparations.

Upon request, all novel materials described in this article will be made available in a timely manner for noncommercial research purposes.

ACKNOWLEDGMENTS

This work was supported by grants from the Biotechnology and Biological Sciences Research Council (BBSRC) and the European Union (Grant CHRX-CT94-0590). P.P. is grateful to the European Union for an Individual Marie Curie fellowship. S.L.H. and L.L.P.-d. are indebted to the BBSRC and the Coordenação de Aperfeiçoamento de Pessoal de Nível Superior for their doctoral studentships.

Received December 20, 2002; accepted February 17, 2003.

REFERENCES

Ahmed, S.U., Rojo, E., Kovaleva, V., Venkataraman, S., Dombrowski, J.E., Matsuoka, K., and Raikhel, N.V. (2000). The plant vacuolar sorting receptor AtELP is involved in transport of NH(2)-terminal propeptide-containing vacuolar proteins in *Arabidopsis thaliana*. J. Cell Biol. **149,** 1335–1344.

Barlowe, C., Orci, L., Yeung, T., Hosobuchi, M., Hamamoto, S., Salama, N., Rexach, M.F., Ravazzola, M., Amherdt, M., and Schekman, R. (1994). COPII: A membrane coat formed by Sec proteins that drive vesicle budding from the endoplasmic reticulum. Cell **77,** 895–907.

Bassham, D.C., and Raikhel, N.V. (2000). Unique features of the plant vacuolar sorting machinery. Curr. Opin. Cell Biol. **12,** 491–495.

Batoko, H., Zheng, H.Q., Hawes, C., and Moore, I. (2000). A rab1 GTPase is required for transport between the endoplasmic reticulum and Golgi apparatus and for normal Golgi movement in plants. Plant Cell **12,** 2201–2218.

Bednarek, S.Y., and Raikhel, N.V. (1991). The barley lectin carboxyl-terminal propeptide is a vacuolar protein sorting determinant in plants. Plant Cell **3,** 1195–1206.

Casadaban, M.J., and Cohen, S.N. (1980). Analysis of gene control signals by DNA fusion and cloning in *Escherichia coli*. J. Mol. Biol. **138,** 179–207.

Chardin, P., and McCormick, F. (1999). Brefeldin A: The advantage of being uncompetitive. Cell **97,** 153–155.

Chardin, P., Paris, S., Antonny, B., Robineau, S., Beraud-Dufour, S., Jackson, C.L., and Chabre, M. (1996). A human exchange factor for ARF contains Sec7- and pleckstrin-homology domains. Nature **384,** 481–484.

Contreras, I., Ortiz-Zapater, E., Castilho, L.M., and Aniento, F. (2000). Characterization of Cop I coat proteins in plant cells. Biochem. Biophys. Res. Commun. **273,** 176–182.

Crofts, A.J., Leborgne-Castel, N., Hillmer, S., Robinson, D.G., Phillipson, B., Carlsson, L.E., Ashford, D.A., and Denecke, J. (1999). Saturation of the endoplasmic reticulum retention machinery reveals anterograde bulk flow. Plant Cell **11,** 2233–2248.

da Silva Conceicao, A., Marty-Mazars, D., Bassham, D.C., Sanderfoot, A.A., Marty, F., and Raikhel, N.V. (1997). The syntaxin homolog AtPEP12p resides on a late post-Golgi compartment in plants. Plant Cell **9,** 571–582.

Denecke, J., Carlsson, L.E., Vidal, S., Hoglund, A.S., Ek, B., van Zeijl, M.J., Sinjorgo, K.M., and Palva, E.T. (1995). The tobacco homolog of mammalian calreticulin is present in protein complexes in vivo. Plant Cell **7,** 391–406.

d'Enfert, C., Gensse, M., and Gaillardin, C. (1992). Fission yeast and a plant have functional homologues of the Sar1 and Sec12 proteins involved in ER to Golgi traffic in budding yeast. EMBO J. **11,** 4205–4211.

Dombrowski, J.E., Schroeder, M.R., Bednarek, S.Y., and Raikhel, N.V. (1993). Determination of the functional elements within the vacuolar targeting signal of barley lectin. Plant Cell **5,** 587–596.

Frigerio, L., de Virgilio, M., Prada, A., Faoro, F., and Vitale, A. (1998). Sorting of phaseolin to the vacuole is saturable and requires a short C-terminal peptide. Plant Cell **10,** 1031–1042.

Geelen, D., Leyman, B., Batoko, H., Di Sansabastiano, G.P., Moore, I., and Blatt, M.R. (2002). The abscisic acid–related SNARE homolog NtSyr1 contributes to secretion and growth: Evidence from competition with its cytosolic domain. Plant Cell **14,** 387–406.

Geldner, N., Anders, N., Wolters, H., Keicher, J., Kornberger, W., Muller, P., Delbarre, A., Ueda, T., Nakano, A., and Jurgens, G. (2003). The Arabidopsis GNOM ARF-GEF mediates endosomal recycling, auxin transport, and auxin-dependent plant growth. Cell **112,** 219–230.

Gomez, L., and Chrispeels, M.J. (1993). Tonoplast and soluble vacuolar proteins are targeted by different mechanisms. Plant Cell **5,** 1113–1124.

Grebe, M., Gadea, J., Steinmann, T., Kientz, M., Rahfeld, J.U., Salchert, K., Koncz, C., and Jurgens, G. (2000). A conserved domain of the Arabidopsis GNOM protein mediates subunit interaction and cyclophilin 5 binding. Plant Cell **12,** 343–356.

Hillmer, S., Movafeghi, A., Robinson, D.G., and Hinz, G. (2001). Vacuolar storage proteins are sorted in the *cis*-cisternae of the pea cotyledon Golgi apparatus. J. Cell Biol. **152,** 41–50.

Hinz, G., Hillmer, S., Baumer, M., and Hohl, I. (1999). Vacuolar storage proteins and the putative vacuolar sorting receptor BP-80 exit the Golgi apparatus of developing pea cotyledons in different transport vesicles. Plant Cell **11,** 1509–1524.

Hoh, B., Hinz, G., Jeong, B.K., and Robinson, D.G. (1995). Protein storage vacuoles form de novo during pea cotyledon development. J. Cell Sci. **108**, 299–310.

Hohl, I., Robinson, D.G., Chrispeels, M.J., and Hinz, G. (1996). Transport of storage proteins to the vacuole is mediated by vesicles without a clathrin coat. J. Cell Sci. **109**, 2539–2550.

Humair, D., Hernandez Felipe, D., Neuhaus, J.M., and Paris, N. (2001). Demonstration in yeast of the function of BP-80, a putative plant vacuolar sorting receptor. Plant Cell **13,** 781–792.

Kirsch, T., Paris, N., Butler, J.M., Beevers, L., and Rogers, J.C. (1994). Purification and initial characterization of a potential plant vacuolar targeting receptor. Proc. Natl. Acad. Sci. USA **91,** 3403–3407.

Kirsch, T., Saalbach, G., Raikhel, N.V., and Beevers, L. (1996). Interaction of a potential vacuolar targeting receptor with amino- and carboxyl-terminal targeting determinants. Plant Physiol. **111,** 469–474.

Koide, Y., Hirano, H., Matsuoka, K., and Nakamura, K. (1997). The N-terminal propeptide of the precursor to sporamin acts as a vacuole-targeting signal even at the C terminus of the mature part in tobacco cells. Plant Physiol. **114,** 863–870.

Koide, Y., Matsuoka, K., Ohto, M., and Nakamura, K. (1999). The N-terminal propeptide and the C terminus of the precursor to 20-kilodalton potato tuber protein can function as different types of vacuolar sorting signals. Plant Cell Physiol. **40,** 1152–1159.

Lee, M.H., Min, M.K., Lee, Y.J., Jin, J.B., Shin, D.H., Kim, D.H., Lee, K.H., and Hwang, I. (2002). ADP-ribosylation factor 1 of Arabidopsis plays a critical role in intracellular trafficking and maintenance of endoplasmic reticulum morphology in Arabidopsis. Plant Physiol. **129,** 1507–1520.

Li, Y.B., Rogers, S.W., Tse, Y.C., Lo, S.W., Sun, S.S., Jauh, G.Y., and Jiang, L. (2002). BP-80 and homologs are concentrated on post-Golgi, probable lytic prevacuolar compartments. Plant Cell Physiol. **43,** 726–742.

Maliga, P., Sz-Breznovits, A., and Marton, L. (1973). Streptomycin-resistant plants from callus culture of haploid tobacco. Nat. New Biol. **244,** 29–30.

Matsuoka, K., Bassham, D.C., Raikhel, N.V., and Nakamura, K. (1995). Different sensitivity to wortmannin of two vacuolar sorting signals indicates the presence of distinct sorting machineries in tobacco cells. J. Cell Biol. **130,** 1307–1318.

Matsuoka, K., and Nakamura, K. (1999). Large alkyl side-chains of isoleucine and leucine in the NPIRL region constitute the core of the vacuolar sorting determinant of sporamin precursor. Plant Mol. Biol. **41,** 825–835.

Matsuoka, K., and Neuhaus, J. (1999). *Cis*-elements of protein transport to the plant vacuoles. J. Exp. Bot. **50,** 165–174.

Melancon, P., Glick, B.S., Malhotra, V., Weidman, P.J., Serafini, T., Gleason, M.L., Orci, L., and Rothman, J.E. (1987). Involvement of GTP-binding "G" proteins in transport through the Golgi stack. Cell **51,** 1053–1062.

Miller, E.A., Lee, M.C., and Anderson, M.A. (1999). Identification and characterization of a prevacuolar compartment in stigmas of *Nicotiana alata*. Plant Cell **11,** 1499–1508.

Moss, J., and Vaughan, M. (1998). Molecules in the ARF orbit. J. Biol. Chem. **273,** 21431–21434.

Movafeghi, A., Happel, N., Pimpl, P., Tai, G.H., and Robinson, D.G. (1999). Arabidopsis Sec21p and Sec23p homologs: Probable coat proteins of plant COP-coated vesicles. Plant Physiol. **119,** 1437–1446.

Murashige, R., and Skoog, F. (1962). A revised medium for rapid growth and bioassays with tobacco tissue cultures. Physiol. Plant. **15,** 473–497.

Neuhaus, J.M., Pietrzak, M., and Boller, T. (1994). Mutation analysis of the C-terminal vacuolar targeting peptide of tobacco chitinase: Low specificity of the sorting system, and gradual transition between intracellular retention and secretion into the extracellular space. Plant J. **5,** 45–54.

Neuhaus, J.M., and Rogers, J.C. (1998). Sorting of proteins to vacuoles in plant cells. Plant Mol. Biol. **38,** 127–144.

Nickel, W., Malsam, J., Gorgas, K., Ravazzola, M., Jenne, N., Helms, J.B., and Wieland, F.T. (1998). Uptake by COPI-coated vesicles of both anterograde and retrograde cargo is inhibited by GTPγS in vitro. J. Cell Sci. **111**, 3081–3090.

Nishikawa, S., Hirata, A., and Nakano, A. (1994). Inhibition of endoplasmic reticulum (ER)-to-Golgi transport induces relocalization of binding protein (BiP) within the ER to form the BiP bodies. Mol. Biol. Cell **5,** 1129–1143.

Paris, N., Stanley, C.M., Jones, R.L., and Rogers, J.C. (1996). Plant cells contain two functionally distinct vacuolar compartments. Cell **85,** 563–572.

Pelham, H.R. (2001). Traffic through the Golgi apparatus. J. Cell Biol. **155,** 1099–1101.

Pelham, H.R., and Rothman, J.E. (2000). The debate about transport in the Golgi: Two sides of the same coin? Cell **102,** 713–719.

Pepperkok, R., Whitney, J.A., Gomez, M., and Kreis, T.E. (2000). COPI vesicles accumulating in the presence of a GTP restricted arf1 mutant are depleted of anterograde and retrograde cargo. J. Cell Sci. **113**, 135–144.

Peyroche, A., Antonny, B., Robineau, S., Acker, J., Cherfils, J., and Jackson, C.L. (1999). Brefeldin A acts to stabilize an abortive ARF-GDP-Sec7 domain protein complex: Involvement of specific residues of the Sec7 domain. Mol. Cell **3,** 275–285.

Pfeffer, S.R. (2001). Membrane transport: Retromer to the rescue. Curr. Biol. **11,** R109–R111.

Phillipson, B.A., Pimpl, P., daSilva, L.L., Crofts, A.J., Taylor, J.P., Movafeghi, A., Robinson, D.G., and Denecke, J. (2001). Secretory bulk flow of soluble proteins is COPII dependent. Plant Cell **13,** 2005–2020.

Pimpl, P., Movafeghi, A., Coughlan, S., Denecke, J., Hillmer, S., and Robinson, D.G. (2000). In situ localization and in vitro induction of plant COPI-coated vesicles. Plant Cell **12,** 2219–2236.

Puertollano, R., Randazzo, P.A., Presley, J.F., Hartnell, L.M., and Bonifacino, J.S. (2001). The GGAs promote ARF-dependent recruitment of clathrin to the TGN. Cell **105,** 93–102.

Ritzenthaler, C., Nebenfuhr, A., Movafeghi, A., Stussi-Garaud, C., Behnia, L., Pimpl, P., Staehelin, L.A., and Robinson, D.G. (2002). Reevaluation of the effects of brefeldin A on plant cells using tobacco Bright Yellow 2 cells expressing Golgi-targeted green fluorescent protein and COPI antisera. Plant Cell **14,** 237–261.

Robinson, D.G., Hinz, G., and Holstein, S.E.H. (1998). The molecular characterization of transport vesicles. Plant Mol. Biol. **38,** 49–76.

Robinson, J.S., Klionsky, D.J., Banta, L.M., and Emr, S.D. (1988). Protein sorting in *Saccharomyces cerevisiae*: Isolation of mutants defective in the delivery and processing of multiple vacuolar hydrolases. Mol. Cell. Biol. **8,** 4936–4948.

Rojo, E., Sharma, V.K., Kovaleva, V., Raikhel, N.V., and Fletcher, J.C. (2002). CLV3 is localized to the extracellular space, where it activates the Arabidopsis CLAVATA stem cell signaling pathway. Plant Cell **14,** 969–977.

Sanderfoot, A.A., Ahmed, S.U., Marty-Mazars, D., Rapoport, I., Kirchhausen, T., Marty, F., and Raikhel, N.V. (1998). A putative vacuolar cargo receptor partially colocalizes with AtPEP12p on a prevacuolar compartment in Arabidopsis roots. Proc. Natl. Acad. Sci. USA **95,** 9920–9925.

Schroeder, M.R., Borkhsenious, O.N., Matsuoka, K., Nakamura, K., and Raikhel, N.V. (1993). Colocalization of barley lectin and sporamin in vacuoles of transgenic tobacco plants. Plant Physiol. **101,** 451–458.

Seaman, M.N., Marcusson, E.G., Cereghino, J.L., and Emr, S.D. (1997). Endosome to Golgi retrieval of the vacuolar protein sorting receptor, Vps10p, requires the function of the VPS29, VPS30, and VPS35 gene products. J. Cell Biol. **137,** 79–92.

Seaman, M.N., McCaffery, J.M., and Emr, S.D. (1998). A membrane coat complex essential for endosome-to-Golgi retrograde transport in yeast. J. Cell Biol. **142,** 665–681.

Shevell, D.E., Kunkel, T., and Chua, N.H. (2000). Cell wall alterations in the Arabidopsis *emb30* mutant. Plant Cell **12,** 2047–2060.

Stamnes, M.A., and Rothman, J.E. (1993). The binding of AP-1 clathrin adaptor particles to Golgi membranes requires ADP-ribosylation factor, a small GTP-binding protein. Cell **73,** 999–1005.

Takeuchi, M., Tada, M., Saito, C., Yashiroda, H., and Nakano, A. (1998). Isolation of a tobacco cDNA encoding Sar1 GTPase and analysis of its dominant mutations in vesicular traffic using a yeast complementation system. Plant Cell Physiol. **39,** 590–599.

Takeuchi, M., Ueda, T., Sato, K., Abe, H., Nagata, T., and Nakano, A. (2000). A dominant negative mutant of Sar1 GTPase inhibits protein transport from the endoplasmic reticulum to the Golgi apparatus in tobacco and Arabidopsis cultured cells. Plant J. **23,** 517–525.

Takeuchi, M., Ueda, T., Yahara, N., and Nakano, A. (2002). Arf1 GTPase plays roles in the protein traffic between the endoplasmic reticulum and the Golgi apparatus in tobacco and Arabidopsis cultured cells. Plant J. **31,** 499–515.

Törmäkangas, K., Hadlington, J.L., Pimpl, P., Hillmer, S., Brandizzi, F., Teeri, T.H., and Denecke, J. (2001). A vacuolar sorting domain may also influence the way in which proteins leave the endoplasmic reticulum. Plant Cell **13,** 2021–2032.

Yahara, N., Ueda, T., Sato, K., and Nakano, A. (2001). Multiple roles of Arf1 GTPase in the yeast exocytic and endocytic pathways. Mol. Biol. Cell **12,** 221–238.